GDCh Research Article Angewandte International Edition Chemie www.angewandte.org

How to cite: *Angew. Chem. Int. Ed.* **2025**, *64*, e202506883
doi.org/10.1002/anie.202506883

Cooperative Catalysis

Acyclic Quaternary Stereocenters via Catalytic Asymmetric Cross-Couplings with Unactivated Alkyl *N*-Hydroxyphthalimide Esters

*Lian-Jie Li, Jun-Chun Zhang, Jia-Yu Tang, Hui Yu, and Ze-Peng Yang**

Abstract: While significant advancements have been made in creating quaternary stereocenters (all-carbon substituents) within cyclic frameworks, generating acyclic quaternary stereocenters poses a more formidable task due to increased conformational flexibility. Herein, we report an enantioselective synthesis of compounds containing acyclic quaternary stereocenters through an iron-catalyzed alkylation reaction between an acyclic tertiary alkyl source and an unactivated primary alkyl source. This method not only facilitates the rapid construction of sterically hindered motifs but also effectively enhances the saturation level of the molecule. Key to this method is an outer-sphere C─C bond formation mechanism, where enantioselectivity is governed by a cooperative triple catalysis system that combines photoredox, chiral Lewis acid, and iron catalysis. A series of compounds featuring acyclic quaternary stereocenters is produced under mild reaction conditions, and various transformations are presented to illustrate the potential applications of this approach. A comprehensive mechanistic study supports the crucial S_H2 (bimolecular homolytic substitution) mechanism.

Introduction

Incorporating quaternary stereocenters (all-carbon substituents) into organic molecules is a valuable strategy for designing bioactive compounds and pharmaceuticals.[1,2] These stereocenters contribute to increased selectivity by broadening the three-dimensional chemical space, allowing for fine-tuning interactions between the drug and its target. For example, among the top 200 small-molecule pharmaceuticals by retail sales in 2023, 19 molecules contain at least one quaternary stereocenter (Scheme 1a).[3] Of these, 15 are steroids, two are chiral lactams, and the remaining two are analogs of Taxol. Like these molecules, the vast majority of organic compounds with quaternary stereocenters are synthesized either from the chiral pool or through chiral resolution methods. Exploiting efficient catalytic asymmetric methods for creating quaternary stereocenters is highly sought after, yet it continues to present a significant challenge in organic synthesis.[4–9] The difficulty arises from substantial steric hindrance, which complicates the approach and alignment of the reacting molecules, thereby hindering the catalyst's efficiency and selectivity in bond formation.

Considerable advances have been achieved in the synthesis of quaternary stereocenters within cyclic structures; however, the formation of acyclic quaternary stereocenters remains a more formidable task due to their greater conformational flexibility.[10–15] The limited number of methods available for creating acyclic quaternary stereocenters is a key factor in the relatively low occurrence of drug molecules with such motifs (Scheme 1a, where all stereocenters in the 19 drug molecules are exclusively cyclic). However, there is a noticeable increase in the emergence of compounds with acyclic quaternary stereocenters that serve as bioactive molecules (Scheme 1b).[16–18] To this end, many catalytic asymmetric strategies have been developed.[19–38] Notably, the intermolecular enantioselective cross-coupling reaction stands out as a modular and versatile approach.[39–51] The alkylation reaction, particularly when employing unactivated alkyl sources, is of great interest due to its potential to rapidly increase the saturation level of a molecule, thus further improving its drug-likeness.[52] However, such reactions are still rare. In 2023, the Tao group realized an elegant Ni-catalyzed α-alkylation reaction of acyclic ketones with unactivated alkyl iodides by utilizing a unique bimetallic ligand (Scheme 1c).[53] However, replacing the methyl group in the ketone with a larger substituent, such as an ethyl group, leads to reduced efficiency and/or selectivity.

In our efforts to develop enantioselective cross-coupling reactions catalyzed by earth-abundant metals, we envisioned that iron would be an ideal metal for the formation of sterically hindered C─C bonds. Unlike typical Ni-catalyzed cross-coupling reactions, which proceed via an inner-sphere reductive elimination mechanism,[54–59] Fe-catalyzed cross-coupling reactions between tertiary alkyl radicals and primary alkyl radicals may follow a bimolecular homolytic substitution (S_H2) pathway through an outer-sphere mechanism.[60–75] There are two main advantages to forming sterically hindered C─C bonds through the iron-mediated outer-sphere

[*] L.-J. Li, J.-C. Zhang, J.-Y. Tang, H. Yu, Z.-P. Yang
Shanghai Key Laboratory of Chemical Assessment and Sustainability, School of Chemical Science and Engineering, Tongji University, Shanghai 200092, P.R China
E-mail: zpyang@tongji.edu.cn

Additional supporting information can be found online in the Supporting Information section

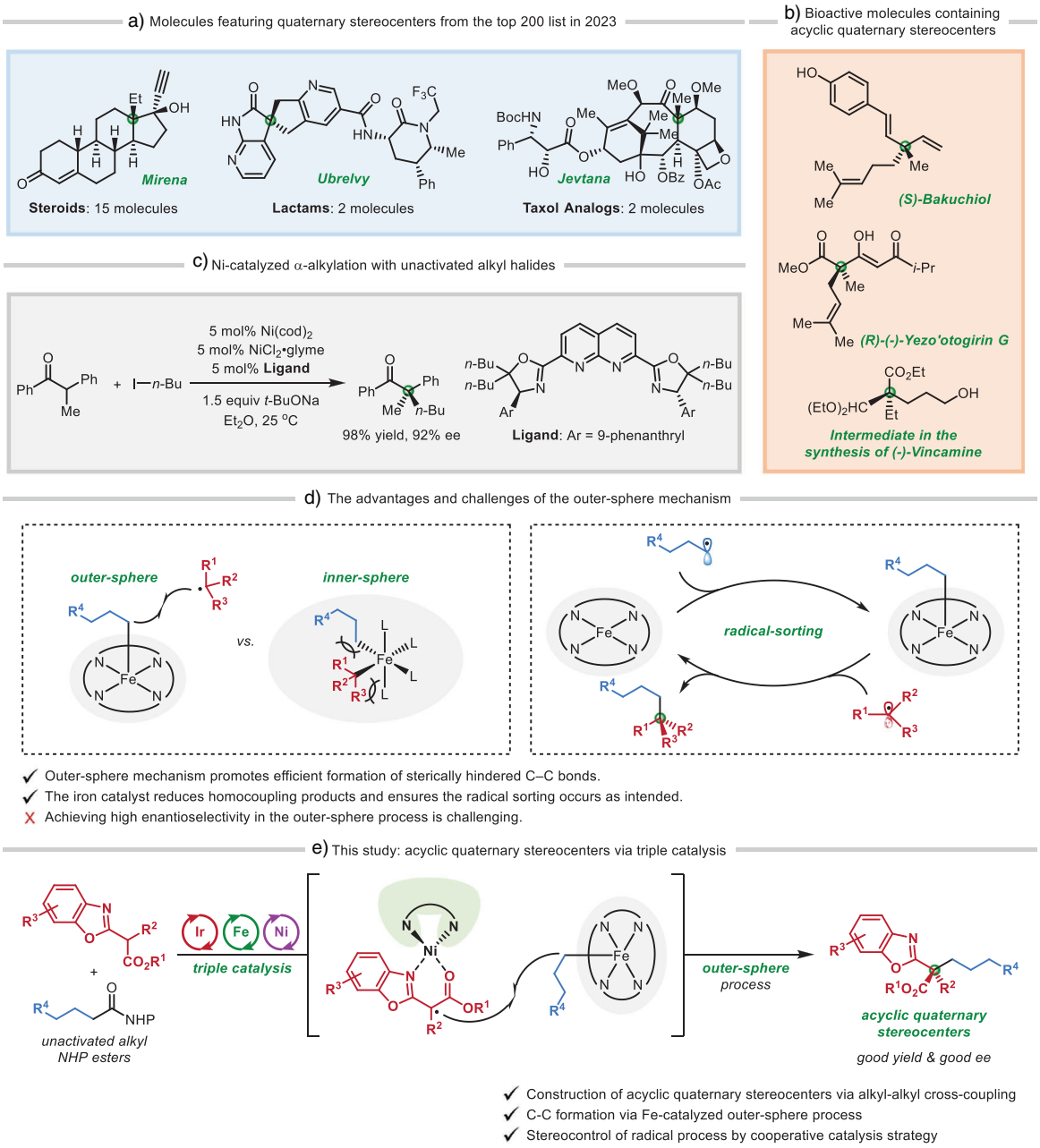

Scheme 1. Background of this study. a) Molecules that contain (cyclic) quaternary stereocenters among the top 200 small-molecule pharmaceuticals by retail sales in 2023. b) Examples of bioactive molecules containing acyclic quaternary stereocenters. c) Nickel-catalyzed α-alkylation reaction of acyclic ketones with unactivated alkyl halides. d) The advantages and challenges of the outer-sphere mechanism. e) This study: acyclic quaternary stereocenters via catalytic asymmetric cross-couplings with unactivated alkyl NHP esters.

mechanism. First, the formation of the C─C bond takes place distal from the metal center, which prevents the formation of sterically hindered tertiary alkyl–metal species and promotes efficient C─C bond formation (Scheme 1d, left). Second, the primary alkyl radical generated is relatively unstable and, upon its formation, readily coordinates with the iron center, resulting in a more stable alkyl–iron species; in contrast, the tertiary alkyl radical is more stable and, once formed, reacts with the alkyl–iron species to generate the C─C bond, thereby minimizing homocoupling side reactions and ensuring the radical sorting proceeds as designed (Scheme 1d, right).[76–81] However, achieving high enantioselectivity during the Fe-catalyzed outer-sphere process is a daunting challenge, with only a few successful examples reported to date. In this context, the Zhang group recently showcased an elegant demonstration of asymmetric olefin cyclopropanation using a chiral iron porphyrin complex.[82,83]

Recently, we realized an enantioselective synthesis of (cyclic) quaternary stereocenters through Fe-catalyzed alkylation reactions facilitated by an outer-sphere

mechanism.[84] However, when acyclic 1,3-dicarbonyl substrates were employed, only moderate yields (31%–34%) were obtained, even when the reaction time was extended to 3 days. Drawing inspiration from the pioneering work of Meggers,[85–88] Feng,[89–92] Xiao,[93–95] Gong,[96–99] Guo,[100–103] and others,[104–107] we envisioned that combining iron catalysis with chiral Lewis acid catalysis would offer an effective platform for the enantioselective construction of highly saturated acyclic quaternary stereocenters. In this article, we present the achievement of this objective that a ternary catalytic system, comprising photocatalysis, iron catalysis, and chiral Lewis acid catalysis, can effectively and selectively promote the coupling of benzoxazolyl acetates with unactivated alkyl NHP (*N*-hydroxyphthalimide) esters under base-free conditions (Scheme 1e).

Results and Discussion

Reaction Optimization

We first investigated the coupling reaction between a benzoxazolyl acetate **1a** and an unactivated alkyl NHP ester **1b** (Table 1).[108] After a comprehensive evaluation of the reaction parameters, we identified that the combination of Fe(OEP)Cl (III, OEP = 2,3,7,8,12,13,17,18-octaethyl-21*H*,23*H*-porphine) and a chiral Lewis acid catalyst, consisting of $Ni(acac)_2$ (acac = acetylacetonate) and (*R*,*S*)-**L1**, can successfully achieve the desired enantioselective cross-coupling in good yield and ee (90% yield, 86% ee; entry 1) under base-free conditions.

The reaction becomes messy in the absence of Fe(OEP)Cl. Although the desired coupling product is still obtained, presumably through a free radical process or an S_H2 process catalyzed by $Ni(acac)_2$,[109,110] both the yield and enantioselectivity are notably reduced (entry 2). Removing the chiral ligand forms a racemic product with decreased efficiency (entry 3). The reaction requires a photocatalyst, a Lewis acid catalyst, or light; otherwise, no product is formed (entry 4). The use of alternative iron catalysts, such as Fe(TPP)Cl (III, TPP = 5,10,15,20-tetraphenyl-21*H*,23*H*-porphyrin), FePc (II, Iron phthalocyanine), or Fe(III) Protoporphyrin IX, as well as other catalysts capable of promoting the S_H2 process, including Vitamin B12, Co(Salen) (II, Salen = *N*,*N*'-bis(salicylidene)ethylenediamine), or Co(TPP) (II), leads to the formation of the product with much lower efficiency and selectivity (entries 5–10). Various other chiral ligands are less effective than (*R*,*S*)-**L1** (entries 11–15). The reaction with a lower amount of Lewis acid catalyst still affords a good yield and enantioselectivity (entry 16). However, the yield decreases when the coupling process is conducted with a lower amount of iron or photocatalyst, for a shorter duration, or at a lower temperature (10 °C), although the ee remains unchanged (entries 17–20). Ethyl acetate is identified as the optimal solvent (entries 21, 22). The reaction proceeds relatively smoothly when a small amount of water is present, whereas a reaction run in the presence of air leads to a diminished yield and ee (entries 23, 24).

Table 1: Catalytic enantioselective cross-coupling of a benzoxazolyl acetate and an unactivated alkyl NHP ester.

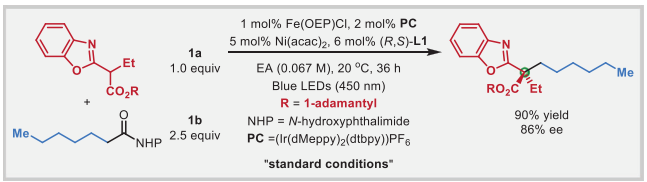

Entry	Variation from the "standard conditions"	Yield (%)[a]	*ee* (%)[b]
1	None	90	86
2	No Fe	20	20
3	No (*R*,*S*)-**L1**	53	0
4	No **PC**, Ni/(*R*,*S*)-**L1**, or light	0	–
5	Fe(TPP)Cl, instead of Fe(OEP)Cl	60	78
6	FePc, instead of Fe(OEP)Cl	22	80
7	Fe(III) Protoporphyrin IX, instead of Fe(OEP)Cl	13	20
8	Vitamin B12, instead of Fe(OEP)Cl	24	17
9	Co(Salen), instead of Fe(OEP)Cl	17	13
10	Co(TPP), instead of Fe(OEP)Cl	0	–
11	**L2**, instead of (*R*,*S*)-**L1**	86	84
12	**L3**, instead of (*R*,*S*)-**L1**	3	–
13	**L4**, instead of (*R*,*S*)-**L1**	56	0
14	**L5**, instead of (*R*,*S*)-**L1**	60	−35
15	**L6**, instead of (*R*,*S*)-**L1**	31	0
16	2.5 mol% $Ni(acac)_2$/3.0 mol% (*R*,*S*)-**L1**	90	83
17	0.5 mol% Fe(OEP)Cl	68	86
18	1.0 mol% **PC**	70	86
19	18 h, instead of 36 h	72	86
20	10 °C, instead of 20 °C	73	86
21	MeCN, instead of EA	0	–
22	$PhCF_3$, instead of EA	8	78
23	1.0 mL air added	34	80
24	1.0 equiv. H_2O added	78	86

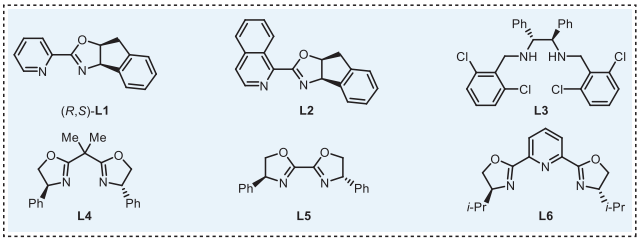

[a] Determined through GC analysis; [b] Determined through HPLC analysis.

Substrate Scope and Applications

With the optimized reaction conditions established, we sought to investigate the generality of substrate scope for both coupling partners. A broad range of unactivated

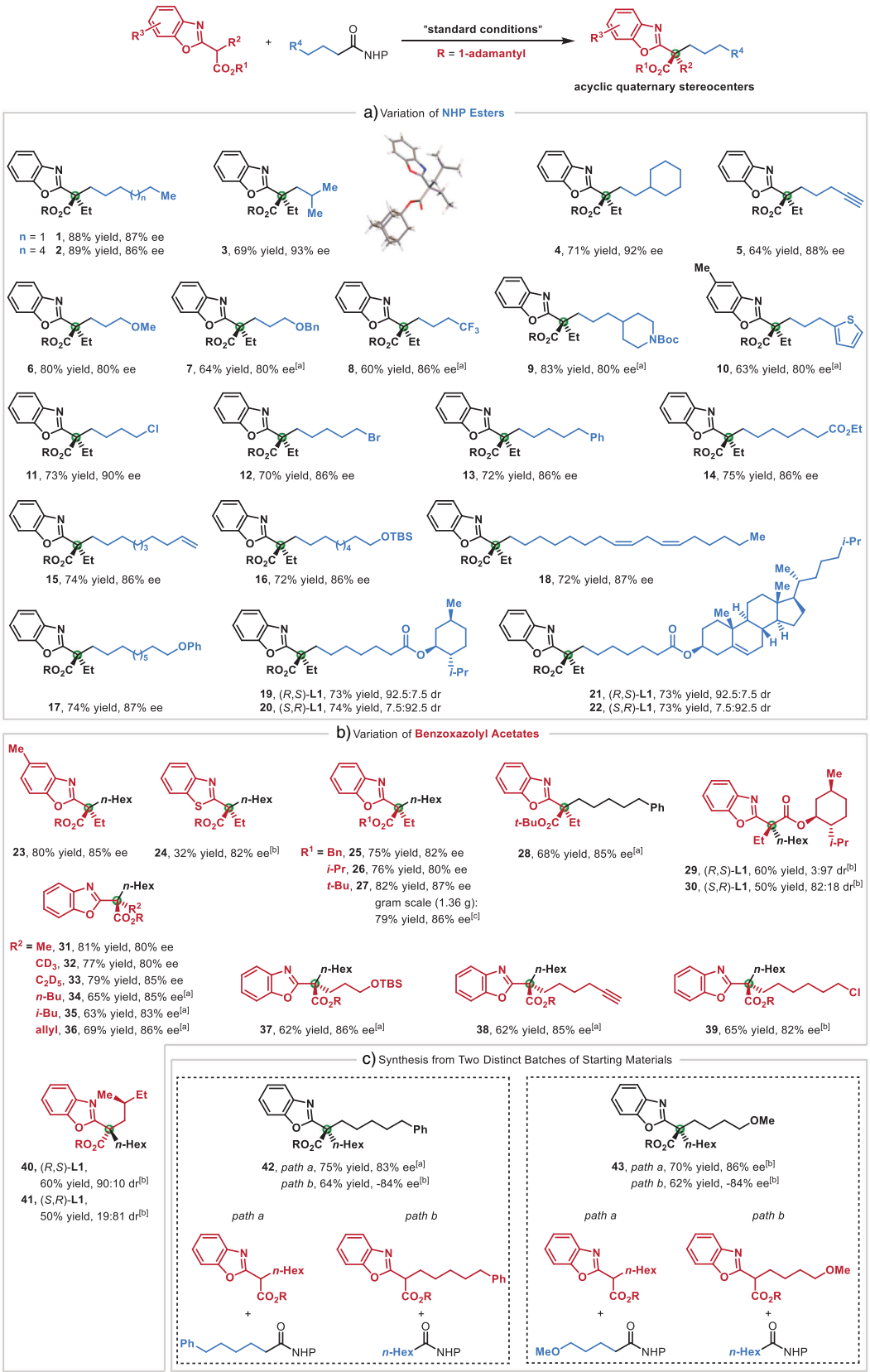

Scheme 2. Scope of the catalytic enantioselective cross-coupling. All couplings were conducted on a 0.20 mmol scale (unless otherwise noted), and all yields are of purified products. a) Variations of NHP esters. b) Variations of benzoxazolyl acetates. c) Synthesis of identical products from two distinct batches of starting materials. [a] The reaction was conducted for 72 h rather than 36 h. [b] The reaction was conducted for 96 h rather than 36 h. [c] The reaction was conducted for 120 h rather than 36 h.

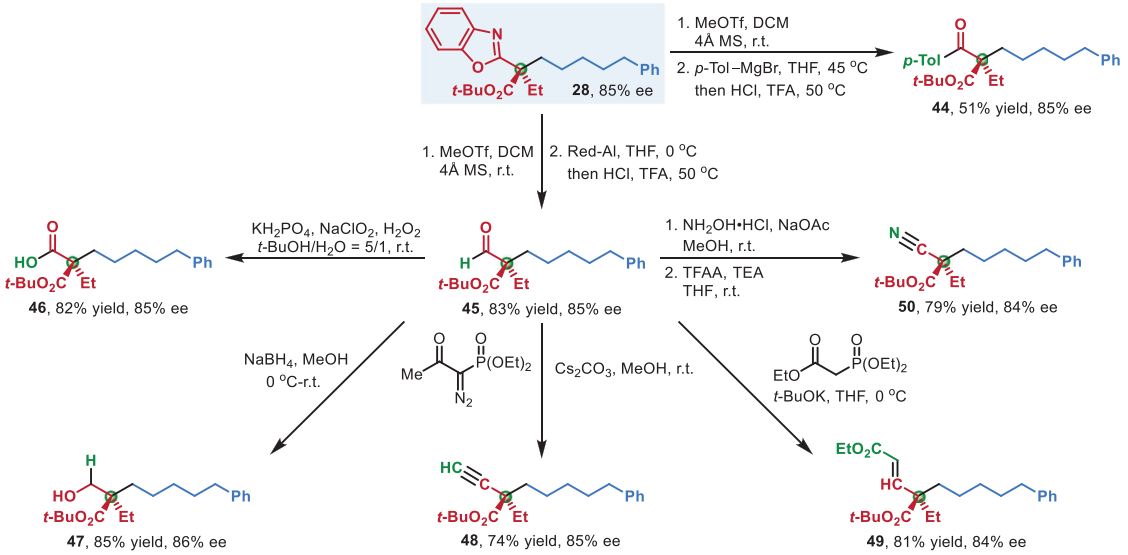

Scheme 3. Transformations into other valuable enantioenriched compounds.

alkyl NHP esters can serve as effective coupling partners in this straightforward photoinduced, iron-catalyzed enantioselective C─C cross-coupling reaction (Scheme 2a). NHP esters bearing various alkyl groups of varying sizes, as well as functional groups such as terminal alkyne, ether, trifluoromethyl, Boc-protected amine, thiophene, unactivated primary alkyl chloride/bromide, ester, terminal/internal alkene, and silyl ether, have proven effective in the formation of acyclic quaternary stereocenters in good yield and enantioselectivity (products **1**–**18**).[111] In the case of an NHP ester possessing stereocenters at a distant position, it is the stereochemistry of the chiral catalyst, rather than that of the chiral NHP ester, that governs the stereochemistry of the coupling product (products **19**–**22**). The absolute configuration of products was unambiguously established through X-ray diffraction analysis of compound **3**.[112]

The scope regarding the benzoxazolyl acetate is also fairly broad (Scheme 2b). Both benzoxazole and benzothiazole rings are suitable for this iron-catalyzed alkylation reaction (products **23**,**24**). The variation in the ester group of benzoxazolyl acetate yields products with high efficiency and enantioselectivity (products **25**–**28**). In the gram-scale synthesis (1.36 g of product), the coupling reaction to produce **27** proceeds with yield and ee almost identical to those observed in the reaction conducted on a 0.20 mmol scale. In the case of benzoxazolyl acetate that bears a chiral ester group, the stereochemistry of the chiral catalyst, rather than that of the benzoxazolyl acetate, controls the stereochemistry of the coupling products (products **29**,**30**). Furthermore, this method efficiently accommodates benzoxazolyl acetates with alkyl substituents ranging in size from methyl to isobutyl, as well as functional groups such as deuterated alkyl, allyl, silyl ether, terminal alkyne, and unactivated primary alkyl chloride, all with good yields and ee values (products **31**–**39**). In reactions involving benzoxazolyl acetates with one stereocenter, the catalyst determines the stereochemistry outcome instead of the substrate (products **40**,**41**).

One advantage of this method is the ability to synthesize an identical product from two distinct permutations of starting materials (Scheme 2c, products **42**,**43**). For example, compound **42** can be obtained via two different synthetic routes: *path a* involves the coupling of *n*-hexyl-substituted benzoxazolyl acetate with phenyl-substituted alkyl NHP ester, while *path b* employs the coupling of phenyl-substituted benzoxazolyl acetate with *n*-hexyl-substituted alkyl NHP ester. Both pathways afford the identical coupling product with high yield and ee, although the resulting stereochemistry is inverted. This flexibility enhances synthetic opportunities, as one can choose the preferred pathway if one route is less favorable. For example, when preparing a coupling product that contains both an ethyl group and an *n*-hexyl group (product **1**), it is recommended to use an *n*-hexyl-substituted NHP ester instead of an ethyl-substituted NHP ester. This is because the coupling reaction with the ethyl-substituted NHP ester produces the product with lower yield and enantioselectivity.[113]

To further demonstrate the synthetic utility of this method, we have transformed the coupling products into a variety of other valuable enantioenriched compounds (Scheme 3). For example, benzoxazole can be readily converted into a ketone or aldehyde (products **44**,**45**). Additionally, the resulting aldehyde serves as a versatile intermediate, enabling direct conversion to various functional groups such as carboxylic acid, alcohol, terminal alkyne, alkene, and nitrile (products **46**–**50**). Notably, no racemization is observed in any of these transformations.

Mechanistic Studies

A series of mechanistic investigations were conducted to gain a deeper understanding of the underlying mechanism. Radical trapping experiments were initially performed to investigate the potential involvement of alkyl radical species

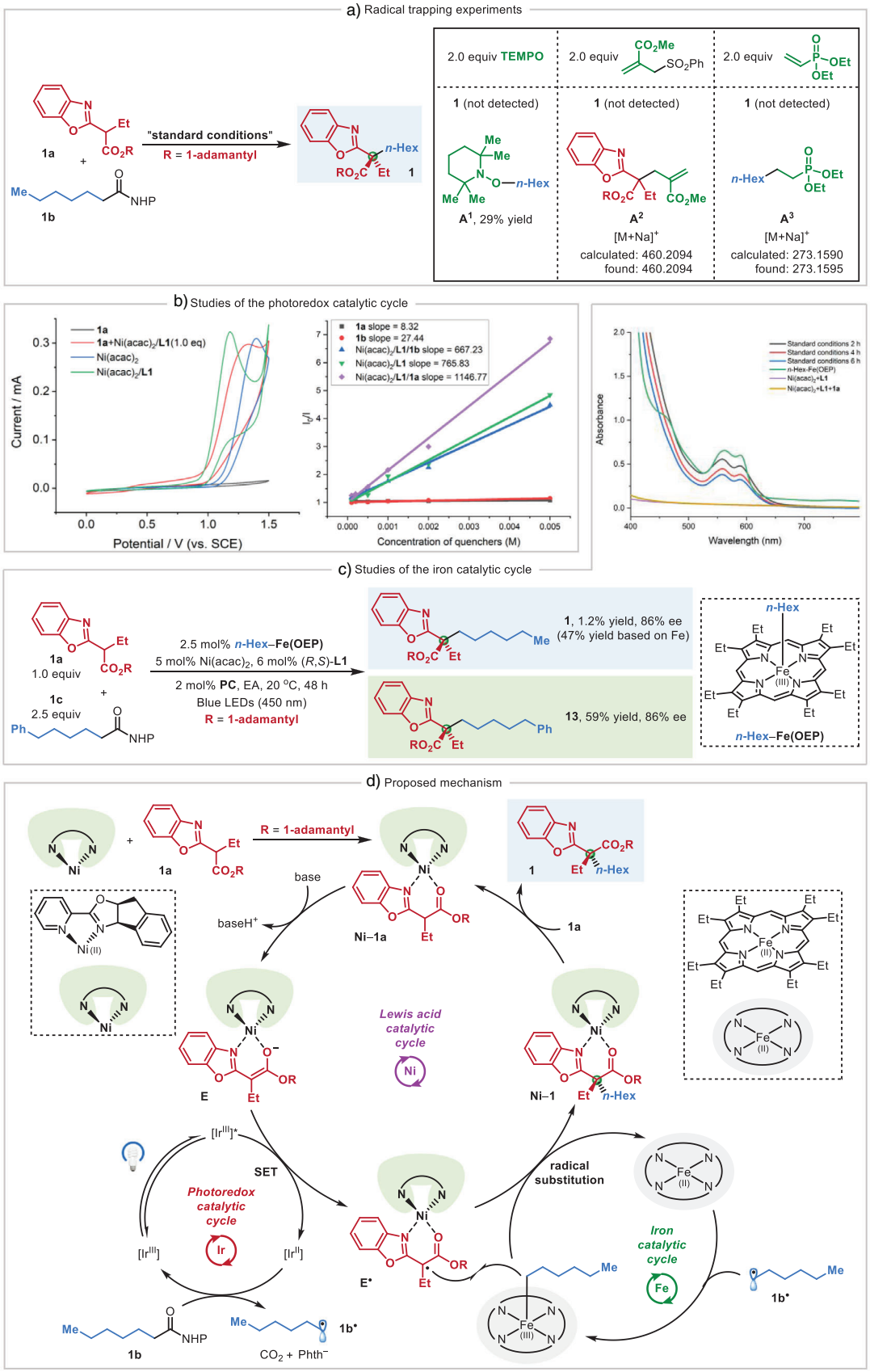

Scheme 4. Mechanism. a) Radical trapping experiments. b) Mechanistic studies of the photoredox catalytic cycle. c) Mechanistic studies of the iron catalytic cycle. d) Outline of a possible catalytic cycle.

in the reaction (Scheme 4a).[114] When 2 equivalents of TEMPO (2,2,6,6-tetramethyl-1-piperidinyloxy) are added to the reaction mixture, the C—C bond formation is completely inhibited, and the TEMPO-adduct **A**^{1} is isolated in 29% yield. Adding 2 equivalents of allylic sulfone or vinyl phosphonate to the model reaction also halts the coupling process, with the adducts **A**^{2} or **A**^{3} detected by high-resolution mass spectrometry. These findings suggest that both **1a** and **1b** could generate alkyl radical species during the coupling reaction.

Cyclic voltammetry (CV) experiments were performed next to elucidate the photoredox catalytic cycle.[115] The onset oxidation potential of **1a** is determined to be +2.04 V versus the saturated calomel electrode (SCE) in acetonitrile (MeCN) (Scheme 4b, left). Upon the introduction of the chiral Lewis acid catalyst, this onset oxidation potential is markedly reduced to +0.36 V versus SCE in MeCN. Additionally, the half-wave potential of **1b** is measured as $E_{1/2}$ (**1b**/**1b**$^{-\bullet}$) = −1.20 V versus SCE in MeCN. The potentials of the photocatalyst (**PC**) are well-established, with the following values: for reductive quenching, $E_{1/2}$ (**PC***/**PC**$^{-}$) = +0.55 V versus SCE in MeCN and $E_{1/2}$ (**PC**/**PC**$^{-}$) = −1.52 V versus SCE in MeCN; for oxidative quenching, $E_{1/2}$ (**PC**$^{+}$/**PC***) = −0.87 V versus SCE in MeCN and $E_{1/2}$ (**PC**$^{+}$/**PC**) = +1.25 V versus SCE in MeCN.[116] While both **PC*** and **PC**$^{+}$ are capable of oxidizing **1a**/Ni/**L1**, only **PC**$^{-}$ is efficient in reducing **1b**, with **PC*** showing limited effectiveness (−0.87 V versus −1.20 V).[117] These findings indicate that the photoinduced electron transfer (PET) process occurs through the reductive quenching pathway.[118] This conclusion is further corroborated by Stern–Volmer studies, which demonstrate that the luminescence of **PC*** is effectively quenched by **1a**/Ni/**L1**, whereas **1b** fails to act as an effective quencher (Scheme 4b, right).

Regarding the iron catalytic cycle, we synthesized the key iron intermediate, the *n*-hexyl-substituted iron complex ***n*-Hex–Fe(OEP)**, to examine the potential involvement of iron species (Scheme 4c).[84] Based on the UV–vis studies, we hypothesized that ***n*-Hex–Fe(OEP)** may be the predominant resting state of the iron catalyst during the coupling reaction. Using 2.5 mol% of five-coordinate ***n*-Hex–Fe(OEP)** as the catalyst, the hexyl transfer product **1** is observed (47% yield based on Fe, 86% ee), providing evidence in support of the proposed S_H2 mechanism. Moreover, the preformed ***n*-Hex–Fe(OEP)** is also able to produce product **13** from the phenylpentyl NHP ester (59% yield, 86% ee), which supports the hypothesis that the alkyl–Fe (III) species is reduced to Fe (II) upon radical substitution, and that the Fe (II) species is proficient in capturing other primary alkyl radical.

Based on the above observations and previous studies, a proposed catalytic cycle for the model reaction is illustrated in Scheme 4d. The reaction begins with the chiral Lewis acid catalyst coordinating to compound **1a**, forming a Ni-bound complex, **Ni–1a**. The enolate species **E** is generated in situ in the presence of a base. Simultaneously, blue light-emitting diode (LED) irradiation activates the iridium photocatalyst [Ir^{III}], promoting the formation of an excited-state complex, [Ir^{III}]*. This complex then oxidizes **E** via PET, yielding reduced [Ir^{II}] and generating a key tertiary alkyl radical, **E**$^{\bullet}$. The reduced [Ir^{II}] acts as a potent reductant, which effectively reduces **1b** to produce a primary alkyl radical, **1b**$^{\bullet}$. In the iron catalytic cycle, **1b**$^{\bullet}$ is captured by a low-valent iron species, Fe(OEP) (II), forming the alkyl–Fe (III) intermediate. A rapid radical substitution occurs between **E**$^{\bullet}$ and alkyl–Fe (III) through an outer-sphere mechanism, producing **Ni–1** and regenerating Fe(OEP) (II). Finally, a ligand substitution releases product **1** containing an acyclic quaternary stereocenter.

Conclusion

We have accomplished an enantioselective synthesis of highly saturated compounds with acyclic quaternary stereocenters through an iron-catalyzed alkylation reaction using unactivated alkyl NHP esters. The efficiency of this sterically demanding construction is dictated by an outer-sphere C—C bond formation mechanism, with enantioselectivity being regulated by a cooperative triple catalysis system that integrates photoredox, chiral Lewis acid, and iron catalysis. This reaction operates under mild, base-free conditions, offering a broad substrate scope and excellent scalability. The resulting coupling products are amenable to further transformations into other valuable compounds containing acyclic quaternary stereocenters. A comprehensive mechanistic study has clarified the reaction pathway, highlighting the crucial S_H2 process. Ongoing efforts in our laboratory are focused on extending iron catalysis to other useful asymmetric reactions.

Supporting Information

The authors have cited additional references within the Supporting Information.[119,120]

Acknowledgements

Support has been provided by the National Natural Science Foundation of China (Grant No. 22201216 to Z.-P.Y.), the National Key Research & Development Program of China (Grant No. 2023YFA1508600 to Z.-P.Y.), and the Fundamental Research Funds for the Central Universities (Grant No. 22120240079 to Z.-P.Y.). The parant organization of the second funding number (2023YFA1508600) should be "Ministry of Science and Technology of the People's Republic of China".

Conflict of Interests

The authors declare no conflict of interest.

Data Availability Statement

The data that support the findings of this study are available in the supplementary material of this article.

Keywords: Cooperative catalysis · Cross-coupling · Iron · Photochemistry · Quaternary stereocenters

[1] T. T. Talele, *J. Med. Chem.* **2018**, *61*, 2166–2210.
[2] T. T. Talele, *J. Med. Chem.* **2020**, *63*, 13291–13315.
[3] J. T. Njardarson, "Top 200 Posters", can be found under https://sites.arizona.edu/njardarson-lab/top200-posters/ (accessed: January 2025).
[4] K. W. Quasdorf, L. E. Overman, *Nature* **2014**, *516*, 181–191.
[5] Y. Liu, S.-J. Han, W.-B. Liu, B. M. Stoltz, *Acc. Chem. Res.* **2015**, *48*, 740–751.
[6] X.-P. Zeng, Z.-Y. Cao, Y.-H. Wang, F. Zhou, J. Zhou, *Chem. Rev.* **2016**, *116*, 7330–7396.
[7] L. Süsse, B. M. Stoltz, *Chem. Rev.* **2021**, *121*, 4084–4099.
[8] P. Xu, F. Zhou, L. Zhu, J. Zhou, *Nat. Synth.* **2023**, *2*, 1020–1036.
[9] Z. Sun, J. Liu, L. Shi, M. Yang, Y. Wang, Y.-P. Han, X. Yao, Y.-M. Liang, *Adv. Synth. Catal.* **2024**, *366*, 4294–4322.
[10] J. P. Das, I. Marek, *Chem. Commun.* **2011**, *47*, 4593.
[11] I. Marek, Y. Minko, M. Pasco, T. Mejuch, N. Gilboa, H. Chechik, J. P. Das, *J. Am. Chem. Soc.* **2014**, *136*, 2682–2694.
[12] J. Feng, M. Holmes, M. J. Krische, *Chem. Rev.* **2017**, *117*, 12564–12580.
[13] B. M. Trost, J. E. Schultz, *Synthesis* **2019**, *51*, 1–30.
[14] D. Pierrot, I. Marek, *Angew. Chem. Int. Ed.* **2020**, *59*, 36–49.
[15] J. Song, X. Li, J. Long, H. Yang, X. Fang, *Chin. J. Chem.* **2024**, *42*, 2485–2498.
[16] Q.-Q. Xu, Q. Zhao, G.-S. Shan, X.-C. Yang, Q.-Y. Shi, X. Lei, *Tetrahedron* **2013**, *69*, 10739–10746.
[17] N. Tanaka, E. Tsuji, Y. Kashiwada, J. Kobayashi, *Chem. Pharm. Bull.* **2016**, *64*, 991–995.
[18] P. Pfäffli, W. Oppolzer, R. Wenger, H. Hauth, *Helv. Chim. Acta* **1975**, *58*, 1131–1145.
[19] A. E. Wendlandt, P. Vangal, E. N. Jacobsen, *Nature* **2018**, *556*, 447–451.
[20] J. C. Green, J. M. Zanghi, S. J. Meek, *J. Am. Chem. Soc.* **2020**, *142*, 1704–1709.
[21] K. Wang, J. Yu, Y. Shao, S. Tang, J. Sun, *Angew. Chem. Int. Ed.* **2020**, *59*, 23516–23520.
[22] Y. Ye, I. Kevlishvili, S. Feng, P. Liu, S. L. Buchwald, *J. Am. Chem. Soc.* **2020**, *142*, 10550–10556.
[23] L. Chen, M. Pu, S. Li, X. Sang, X. Liu, Y.-D. Wu, X. Feng, *J. Am. Chem. Soc.* **2021**, *143*, 19091–19098.
[24] M. G. J. Doyle, A. L. Gabbey, W. McNutt, R. J. Lundgren, *Angew. Chem. Int. Ed.* **2021**, *60*, 26495–26499.
[25] C. Hervieu, M. S. Kirillova, T. Suárez, M. Müller, E. Merino, C. Nevado, *Nat. Chem.* **2021**, *13*, 327–334.
[26] M. Isomura, D. A. Petrone, E. M. Carreira, *J. Am. Chem. Soc.* **2021**, *143*, 3323–3329.
[27] X. Liu, C. Zhao, R. Zhu, L. Liu, *Angew. Chem. Int. Ed.* **2021**, *60*, 18499–18503.
[28] K. Ohmatsu, Y. Morita, M. Kiyokawa, T. Ooi, *J. Am. Chem. Soc.* **2021**, *143*, 11218–11224.
[29] J. Wang, F. He, X. Yang, *Nat. Commun.* **2021**, *12*, 6700.
[30] F. A. Moghadam, E. F. Hicks, Z. P. Sercel, A. Q. Cusumano, M. D. Bartberger, B. M. Stoltz, *J. Am. Chem. Soc.* **2022**, *144*, 7983–7987.
[31] P. Xu, S. Liu, Z. Huang, *J. Am. Chem. Soc.* **2022**, *144*, 6918–6927.
[32] J. Dai, L. Li, R. Ye, S. Wang, Y. Wang, F. Peng, Z. Shao, *Angew. Chem. Int. Ed.* **2023**, *62*, e202300756.
[33] J. Shen, Z. Xu, S. Yang, S. Li, J. Jiang, Y.-Q. Zhang, *J. Am. Chem. Soc.* **2023**, *145*, 21122–21131.
[34] J. Song, W.-H. Zheng, *J. Am. Chem. Soc.* **2023**, *145*, 8338–8343.
[35] J. Wei, V. Gandon, Y. Zhu, *J. Am. Chem. Soc.* **2023**, *145*, 16796–16811.
[36] G. Zhang, M. D. Wodrich, N. Cramer, *Science* **2024**, *383*, 395–401.
[37] K. Chen, S. Zhou, C. Li, S. Dong, K. Hong, X. Xu, *J. Am. Chem. Soc.* **2024**, *146*, 19261–19270.
[38] Y. Yang, J. Chen, Y. Shi, P. Liu, Y. Feng, Q. Peng, S. Xu, *J. Am. Chem. Soc.* **2024**, *146*, 1635–1643.
[39] L. Næsborg, L. A. Leth, G. J. Reyes-Rodríguez, T. A. Palazzo, V. Corti, K. A. Jørgensen, *Chem.-Eur. J.* **2018**, *24*, 14844–14848.
[40] X.-W. Chen, L. Zhu, Y.-Y. Gui, K. Jing, Y.-X. Jiang, Z.-Y. Bo, Y. Lan, J. Li, D.-G. Yu, *J. Am. Chem. Soc.* **2019**, *141*, 18825–18835.
[41] L. A. Schwartz, M. Holmes, G. A. Brito, T. P. Gonçalves, J. Richardson, J. C. Ruble, K.-W. Huang, M. J. Krische, *J. Am. Chem. Soc.* **2019**, *141*, 2087–2096.
[42] S. Feng, S. L. Buchwald, *J. Am. Chem. Soc.* **2021**, *143*, 4935–4941.
[43] Z. Wang, Z.-P. Yang, G. C. Fu, *Nat. Chem.* **2021**, *13*, 236–242.
[44] S.-L. Zhang, W.-W. Zhang, B.-J. Li, *J. Am. Chem. Soc.* **2021**, *143*, 9639–9647.
[45] C.-F. Liu, Z.-C. Wang, X. Luo, J. Lu, C. H. M. Ko, S.-L. Shi, M. J. Koh, *Nat. Catal.* **2022**, *5*, 934–942.
[46] Y.-F. Cheng, Z.-L. Yu, Y. Tian, J.-R. Liu, H.-T. Wen, N.-C. Jiang, J.-Q. Bian, G.-X. Xu, D.-T. Xu, Z.-L. Li, Q.-S. Gu, X. Hong, X.-Y. Liu, *Nat. Chem.* **2023**, *15*, 395–404.
[47] D. Ghorai, A. Garcia-Roca, B. L. Tóth, J. Benet-Buchholz, A. W. Kleij, *Angew. Chem. Int. Ed.* **2023**, *62*, e202314865.
[48] Y.-Y. Gui, X.-W. Chen, X.-Y. Mo, J.-P. Yue, R. Yuan, Y. Liu, L.-L. Liao, J.-H. Ye, D.-G. Yu, *J. Am. Chem. Soc.* **2024**, *146*, 2919–2927.
[49] W. Huang, Y. Xi, D. Pan, L. Fan, K. Fang, G. Huang, W.-H. Zhu, J. Qu, Y. Chen, *J. Am. Chem. Soc.* **2024**, *146*, 16892–16901.
[50] X. Luo, W. Mao, C.-F. Liu, Y.-Q. Wang, J. Nie, S.-L. Shi, J.-A. Ma, M. J. Koh, *Nat. Synth.* **2024**, *3*, 633–642.
[51] S. Zhang, L. Li, D. Li, Y.-Y. Zhou, Y. Tang, *J. Am. Chem. Soc.* **2024**, *146*, 2888–2894.
[52] F. Lovering, J. Bikker, C. Humblet, *J. Med. Chem.* **2009**, *52*, 6752–6756.
[53] P. Wang, L. Zhu, J. Wang, Z. Tao, *J. Am. Chem. Soc.* **2023**, *145*, 27211–27217.
[54] A. H. Cherney, N. T. Kadunce, S. E. Reisman, *Chem. Rev.* **2015**, *115*, 9587–9652.
[55] T. Iwasaki, N. Kambe, *Top. Curr. Chem.* **2016**, *374*, 66.
[56] G. C. Fu, *ACS Cent. Sci.* **2017**, *3*, 692–700.
[57] J. Choi, G. C. Fu, *Science* **2017**, *356*, eaaf7230.
[58] A. Kaga, S. Chiba, *ACS Catal.* **2017**, *7*, 4697–4706.
[59] G. A. Dawson, E. H. Spielvogel, T. Diao, *Acc. Chem. Res.* **2023**, *56*, 3640–3653.
[60] W. Liu, M. N. Lavagnino, C. A. Gould, J. Alcázar, D. W. C. MacMillan, *Science* **2021**, *374*, 1258–1263.
[61] X.-C. Gan, S. Kotesova, A. Castanedo, S. A. Green, S. L. B. Møller, R. A. Shenvi, *J. Am. Chem. Soc.* **2023**, *145*, 15714–15720.
[62] C. A. Gould, A. L. Pace, D. W. C. MacMillan, *J. Am. Chem. Soc.* **2023**, *145*, 16330–16336.
[63] X.-C. Gan, B. Zhang, N. Dao, C. Bi, M. Pokle, L. Kan, M. R. Collins, C. C. Tyrol, P. N. Bolduc, M. Nicastri, Y. Kawamata, P. S. Baran, R. Shenvi, *Science* **2024**, *384*, 113–118.
[64] L. Kong, X.-C. Gan, V. A. van der Puyl Lovett, R. A. Shenvi, *J. Am. Chem. Soc.* **2024**, *146*, 2351–2357.
[65] A. L. Pace, F. Xu, W. Liu, M. N. Lavagnino, D. W. C. MacMillan, *J. Am. Chem. Soc.* **2024**, *146*, 32925–32932.
[66] T.-D. Tan, J. M. I. Serviano, X. Luo, P.-C. Qian, P. L. Holland, X. Zhang, M. J. Koh, *Nat. Catal.* **2024**, *7*, 321–329.
[67] Q. Zhang, S. Wu, X. Wu, *Green Chem.* **2024**, *26*, 11334–11339.

[68] J. Xie, P. Xu, Y. Zhu, J. Wang, W.-C. C. Lee, X. P. Zhang, *J. Am. Chem. Soc.* **2021**, *143*, 11670–11678.
[69] C. Zhang, D.-S. Wang, W.-C. C. Lee, A. M. McKillop, X. P. Zhang, *J. Am. Chem. Soc.* **2021**, *143*, 11130–11140.
[70] J. Ke, W.-C. C. Lee, X. Wang, Y. Wang, X. Wen, X. P. Zhang, *J. Am. Chem. Soc.* **2022**, *144*, 2368–2378.
[71] Z. Jia, L. Zhang, S. Luo, *J. Am. Chem. Soc.* **2022**, *144*, 10705–10710.
[72] W.-C. C. Lee, J. Wang, Y. Zhu, X. P. Zhang, *J. Am. Chem. Soc.* **2023**, *145*, 11622–11632.
[73] A. V. Tsymbal, L. D. Bizzini, D. W. C. MacMillan, *J. Am. Chem. Soc.* **2022**, *144*, 21278–21286.
[74] E. Mao, D. W. C. MacMillan, *J. Am. Chem. Soc.* **2023**, *145*, 2787–2793.
[75] F. Cong, G.-Q. Sun, S.-H. Ye, R. Hu, W. Rao, M. J. Koh, *J. Am. Chem. Soc.* **2024**, *146*, 10274–10280.
[76] A. Vasilopoulos, S. W. Krska, S. S. Stahl, *Science* **2021**, *372*, 398–403.
[77] B. Zhang, Y. Gao, Y. Hioki, M. S. Oderinde, J. X. Qiao, K. X. Rodriguez, H.-J. Zhang, Y. Kawamata, P. S. Baran, *Nature* **2022**, *606*, 313–318.
[78] H. A. Sakai, D. W. C. MacMillan, *J. Am. Chem. Soc.* **2022**, *144*, 6185–6192.
[79] Q. Cai, I. M. McWhinnie, N. W. Dow, A. Y. Chan, D. W. C. MacMillan, *J. Am. Chem. Soc.* **2024**, *146*, 12300–12309.
[80] J. Z. Wang, W. L. Lyon, D. W. C. MacMillan, *Nature* **2024**, *628*, 104–109.
[81] J. Z. Wang, E. Mao, J. A. Nguyen, W. L. Lyon, D. W. C. MacMillan, *J. Am. Chem. Soc.* **2024**, *146*, 15693–15700.
[82] W.-C. C. Lee, D.-S. Wang, Y. Zhu, X. P. Zhang, *Nat. Chem.* **2023**, *15*, 1569–1580.
[83] For an elegant Cu-catalyzed enantioconvergent cross-coupling of tertiary electrophiles, see: F.-L. Wang, C.-J. Yang, J.-R. Liu, N.-Y. Yang, X.-Y. Dong, R.-Q. Jiang, X.-Y. Chang, Z.-L. Li, G.-X. Xu, D.-L. Yuan, Y.-S. Zhang, Q.-S. Gu, X. Hong, X.-Y. Liu, *Nat. Chem.* **2022**, *14*, 949–957.
[84] L.-J. Li, J.-C. Zhang, W.-P. Li, D. Zhang, K. Duanmu, H. Yu, Q. Ping, Z.-P. Yang, *J. Am. Chem. Soc.* **2024**, *146*, 9404–9412.
[85] H. Huo, X. Shen, C. Wang, L. Zhang, P. Röse, L.-A. Chen, K. Harms, M. Marsch, G. Hilt, E. Meggers, *Nature* **2014**, *515*, 100–103.
[86] X. Huang, R. D. Webster, K. Harms, E. Meggers, *J. Am. Chem. Soc.* **2016**, *138*, 12636–12642.
[87] X. Huang, Q. Zhang, J. Lin, K. Harms, E. Meggers, *Nat. Catal.* **2019**, *2*, 34–40.
[88] P. Xiong, M. Hemming, S. I. Ivlev, E. Meggers, *J. Am. Chem. Soc.* **2022**, *144*, 6964–6971.
[89] X. Zhang, W. Wu, W. Cao, H. Yu, X. Xu, X. Liu, X. Feng, *Angew. Chem. Int. Ed.* **2020**, *59*, 4846–4850.
[90] Y. Luo, Q. Wei, L. Yang, Y. Zhou, W. Cao, Z. Su, X. Liu, X. Feng, *ACS Catal.* **2022**, *12*, 12984–12992.
[91] Y. Luo, Y. Zhou, F. Xiao, X. He, Z. Zhong, Q.-L. Zhou, W. Cao, X. Liu, X. Feng, *ACS Catal.* **2024**, *14*, 12031–12041.
[92] N. Xu, M. Pu, H. Yu, G. Yang, X. Liu, X. Feng, *Angew. Chem. Int. Ed.* **2024**, *63*, e202314256.
[93] X.-S. Zhou, Z. Zhang, W.-Y. Qu, X.-P. Liu, W.-J. Xiao, M. Jiang, J.-R. Chen, *J. Am. Chem. Soc.* **2023**, *145*, 12233–12243.
[94] Y. Jia, K. Zhang, L.-Q. Lu, Y. Cheng, W.-J. Xiao, *ACS Catal.* **2024**, *14*, 13550–13556.
[95] W.-Y. Qu, X.-S. Zhou, W.-J. Xiao, J.-R. Chen, *Sci. Chi. Chem.* **2024**, *67*, 3807–3816.
[96] Y. Li, K. Zhou, Z. Wen, S. Cao, X. Shen, M. Lei, L. Gong, *J. Am. Chem. Soc.* **2018**, *140*, 15850–15858.
[97] Y. Li, M. Lei, L. Gong, *Nat. Catal.* **2019**, *2*, 1016–1026.
[98] S. Cao, W. Hong, Z. Ye, L. Gong, *Nat. Commun.* **2021**, *12*, 2377.
[99] Z. Chi, J.-B. Liao, X. Cheng, Z. Ye, W. Yuan, Y.-M. Lin, L. Gong, *J. Am. Chem. Soc.* **2024**, *146*, 10857–10867.
[100] Q. Zhang, X. Chang, L. Peng, C. Guo, *Angew. Chem. Int. Ed.* **2019**, *58*, 6999–7003.
[101] K. Liang, Q. Zhang, C. Guo, *Nat. Synth.* **2023**, *2*, 1184–1193.
[102] J. Zhang, W. Zhu, Z. Chen, Q. Zhang, C. Guo, *J. Am. Chem. Soc.* **2024**, *146*, 1522–1531.
[103] J. Li, M. Liu, B. Wei, L. Peng, J. Song, C. Guo, *J. Am. Chem. Soc.* **2024**, *146*, 34043–34052.
[104] L. R. Espelt, I. S. McPherson, E. M. Wiensch, T. P. Yoon, *J. Am. Chem. Soc.* **2015**, *137*, 2452–2455.
[105] A. G. Amador, E. M. Sherbrook, T. P. Yoon, *J. Am. Chem. Soc.* **2016**, *138*, 4722–4725.
[106] S. Cao, D. Kim, W. Lee, S. Hong, *Angew. Chem. Int. Ed.* **2023**, *62*, e202312780.
[107] Y. Tao, W. Ma, R. Sun, C. Huang, Q. Lu, *Angew. Chem. Int. Ed.* **2024**, *63*, e202409222.
[108] For more details, please see section IV of the Supporting Information.
[109] R. Chen, N. E. Intermaggio, J. Xie, J. A. Rossi-Ashton, C. A. Gould, R. T. Martin, J. Alcázar, D. W. C. MacMillan, *Science* **2024**, *383*, 1350–1357.
[110] W. L. Lyon, J. Z. Wang, J. Alcázar, D. W. C. MacMillan, *J. Am. Chem. Soc.* **2025**, *147*, 2296–2302.
[111] We assessed the fate of the NHP ester in the coupling reaction that produces compound **13**. Notably, a significant amount of the decarbonyl compound 2-(5-phenylpentyl)isoindoline-1,3-dione is observed, yielding 35% based on the NHP ester. Furthermore, GC analysis indicates the presence of a small quantity of hydro-dephthalimide product related to the NHP ester.
[112] Deposition number 2410484 (for **3**) contains the supplementary crystallographic data for this paper. These data are provided free of charge by the joint Cambridge Crystallographic Data Centre and Fachinformationszentrum Karlsruhe Access Structures service.
[113] For examples of unsuccessful attempts in this coupling reaction, please see section V of the Supporting Information.
[114] Q. Zhang, J. Zhang, W. Zhu, R. Lu, C. Guo, *Nat. Commun.* **2024**, *15*, 4477.
[115] For details, please see section VII of the Supporting Information.
[116] J. A. Terrett, M. D. Clift, D. W. C. MacMillan, *J. Am. Chem. Soc.* **2014**, *136*, 6858–6861.
[117] An alternative possibility is that Fe(II) is reduced by $\mathbf{PC}^-$ to form Fe(I), which then reduces **1b**, leading to the formation of **1b–•** and the regeneration of Fe(II).
[118] N. A. Romero, D. A. Nicewicz, *Chem. Rev.* **2016**, *116*, 10075–10166.
[119] D. Sahoo, M. G. Quesne, S. P. de Visser, S. P. Rath, *Angew. Chem. Int. Ed.* **2015**, *54*, 4796–4800.
[120] X. Chang, J. Zhang, X. Cheng, X. Lv, C. Guo, *Adv. Sci.* **2024**, *11*, 2406764.

Manuscript received: March 26, 2025
Revised manuscript received: April 05, 2025
Accepted manuscript online: April 05, 2025
Version of record online: April 17, 2025